ISSN 0030-400X, Optics and Spectroscopy, 2015, Vol. 118, No. 6, pp. 978–987. © Pleiades Publishing, Ltd., 2015.
Original Russian Text © A.V. Kalenskii, A.A. Zvekov, A.P. Nikitin, M.V. Anan'eva, B.P. Aduev, 2015, published in Optika i Spektroskopiya, 2015, Vol. 118, No. 6, pp. 1012–1021.

PHYSICAL OPTICS

Specific Features of Plasmon Resonance in Nanoparticles of Different Metals

A. V. Kalenskii[a], A. A. Zvekov[b], A. P. Nikitin[b], M. V. Anan'eva[a], and B. P. Aduev[b]

[a] *Kemerovo State University, Krasnaya ul. 6, Kemerovo, 650043 Russia*

[b] *Institute of Coal Chemistry and Material Science, Siberian Branch, Russian Academy of Sciences, Sovetskii pr. 18, Kemerovo, 650000 Russia*

e-mail: kriger@kemsu.ru

Received December 15, 2014

Abstract—Spectral dependences of the light extinction and absorption efficiency coefficients are calculated for silver, gold, nickel, and aluminum nanoparticles within the framework of the Mie theory. It is demonstrated that narrow plasmon bands are observed for small (with a radius of less than 50 nm) nanoparticles of noble metals, whereas broad bands in the spectral dependences of the extinction and absorption efficiencies are typical for nickel and aluminum nanoparticles. It is concluded that using spectral dependences of extinction for estimating the radius of nanoparticles is correct only for noble metals. The results are interpreted based on wavelength dependences of complex refractive indices of metals.

DOI: 10.1134/S0030400X15060119

INTRODUCTION

Currently, there is a great interest in the investigation of the optical properties of nanoparticles, because they are used in a large number of technical applications. It has been suggested to use metal nanoparticles in nonlinear optical devices [1–7]. It has been shown that introduction of noble metal nanoparticles (gold [1, 2], silver [3–5], and copper [3, 6, 7]) into different matrices leads to the index of refraction and coefficient of absorption becoming dependent on laser radiation power. It was noted in [3] that the introduction of metal nanoparticles improves nonlinear optical properties of such materials as lithium niobate. Enhancement of an oscillating electromagnetic field in the vicinity of nanoparticles or nanoscale irregularities of surface relief as a result of their interaction with the electromagnetic wave [8, 9] can be used for detecting trace amounts of substances by means of Raman spectroscopy [9]. It was proposed to introduce metal nanoparticles into solar cells for increasing their efficiency by reducing reflectivity [10]. Introduction of nanoscale carbon particles allows increasing efficiency of solar heaters due to increased coefficient of absorption [11]. Using metal nanoparticles for hyperthermal cancer therapy, wherein nanoparticles are introduced into the body, decorate tumors and are subsequently heated by laser radiation, thus killing cancer cells, is currently under investigation [12, 13]. Introduction of metal nanoparticles for increasing the sensitivity of brisant explosives to laser radiation was reported in [14–18]. It has been concluded that such nanocomposites are promising materials that can be used in capsules of optical detonators [18].

In all above cases, the operational efficiency of a device is determined by optical properties of nanoparticles, which depend on their composition, size, shape, and radiation wavelength. In most cases, when discussing experimental results and predicting the efficiency of operation of a specific device, the concept of plasmon resonance associated with local maximum in the spectral dependence of the extinction coefficient of the substance containing nanoparticles is used. Spectral dependences of extinction of noble metal nanoparticles in the vicinity of plasmon resonance band were measured experimentally in a large number of studies, although the question about specificities of plasmon resonance in other metals remains open.

This work aims at studying plasmon resonance in nanoparticles of different metals. We set the goal of calculating coefficients of extinction, absorption, and scattering efficiency for gold, silver, nickel, and aluminum nanoparticles as functions of their radius and radiation wavelength. Selection of metals was dictated by the fact that silver and gold represent typical noble metals exhibiting high conductivity and chemical resistivity, whereas nickel belongs to metals of the iron subgroup exhibiting lower conductivity. Aluminum occupies an intermediate position, combining high conductivity with chemical activity.

Table 1. Calculated position and amplitude of peaks in the spectral dependence of absorption, scattering, and extinction efficiency coefficients for silver and gold nanoparticles of different radii

R, nm	Silver						Gold					
	λ_1, nm	Q_1	λ_2, nm	Q_2	λ_3, nm	Q_3	λ_1, nm	Q_1	λ_2, nm	Q_2	λ_3, nm	Q_3
10.0	425.1	16.44	425.3	3.15	425.2	19.58	527.7	2.36	534.2	0.04	527.8	2.39
12.5	428.6	15.85	428.9	6.03	428.7	21.87	528.8	2.97	535.2	0.10	529.0	3.06
15.0	432.8	13.51	433.1	9.08	432.9	22.58	530.2	3.58	536.5	0.20	530.6	3.77
17.5	437.6	10.54	438.1	11.50	437.9	22.04	531.8	4.14	538.0	0.38	532.4	4.50
20.0	443.0	7.78	443.6	12.95	443.4	20.72	533.7	4.62	539.8	0.66	534.5	5.24
22.5	448.9	5.57	449.8	13.50	449.5	19.06	535.8	4.97	542.0	1.05	537.0	5.97
25.0	455.3	3.95	456.4	13.41	456.2	17.34	538.1	5.16	544.5	1.56	539.7	6.64
27.5	462.1	2.81	463.6	12.90	463.3	15.70	540.5	5.16	547.4	2.16	542.7	7.22
30.0	469.3	2.03	471.1	12.20	470.9	14.22	543.2	4.98	550.8	2.82	546.1	7.67
32.5	476.8	1.49	479.1	11.44	478.9	12.92	545.9	4.64	554.7	3.49	550.0	7.99
35.0	485.2	1.11	487.4	10.67	487.2	11.78	548.8	4.21	559.4	4.12	554.3	8.16
37.5	494.1	0.85	496.0	9.94	495.9	10.79	551.5	3.72	564.9	4.69	559.2	8.21
40.0	504.0	0.67	504.9	9.26	504.9	9.93	553.8	3.24	570.9	5.18	564.8	8.17
42.5	417.4	2.90	514.2	8.65	514.2	9.18	555.0	2.79	577.4	5.56	570.9	8.06
45	420.9	2.71	523.9	8.10	524.0	8.54	529.3	2.40	584.1	5.84	577.4	7.89
47.5	424.7	2.46	534.3	7.61	425.3	8.28	524.6	2.27	590.9	6.00	584.4	7.68
50	428.7	2.18	545.3	7.18	429.4	8.40	523.2	2.19	597.4	6.07	591.5	7.43

METHOD OF CALCULATION

It was demonstrated in [19] that the concept of plasmon resonance does not contradict the Mie theory. Therefore, we conducted all calculations within the framework of the latter, wherein the coefficients of extinction efficiency (Q_{ext}) and scattering efficiency (Q_{sca}) of light with a given wavelength λ by spherical inclusion of radius R are calculated straightforward. These quantities are defined as the ratio of the corresponding cross section to the geometrical cross section of the sphere πR^2. For convenience of analysis of the results, expressions for extinction and scattering efficiency coefficients are presented in the form

$$Q_{ext} = \sum_{l=1}^{\infty}\left(F^c_{l\,ext} + F^b_{l\,ext}\right), \quad (1)$$

$$Q_{sca} = \sum_{l=1}^{\infty}\left(F^c_{l\,sca} + F^b_{l\,sca}\right). \quad (2)$$

The coefficient of light absorption (Q_{abs}) is calculated as the difference of the coefficients of extinction and scattering efficiency: $Q_{abs} = Q_{ext} - Q_{sca}$ [16, 17, 19–21]. The quantities in parentheses corresponding to the contributions of electric, F^c_l, and magnetic, F^b_l, oscillations to each of the efficiency coefficients are given by

$$F^c_{l\,ext} = (2/\rho^2)(2l+1)|c_l|^2, \quad (3a)$$

$$F^b_{l\,ext} = (2/\rho^2)(2l+1)|b_l|^2, \quad (3b)$$

$$F^c_{l\,sca} = (2/\rho^2)(2l+1)\,\mathrm{Im}\,c_l, \quad (3c)$$

$$F^b_{l\,sca} = -(2/\rho^2)(2l+1)\,\mathrm{Im}\,b_l, \quad (3d)$$

where $\rho = 2\pi R m_0/\lambda$ is the dimensionless radius of the nanoparticle and m_0 is the refractive index of the medium. In the simulation, we assumed that $m_0 = 1.5$, because this is a typical value for dielectric media. In addition, the refractive index of hexogen is 1.5. Therefore, some of the results can be used for predicting properties of optical detonators based on hexogen with metal nanoparticles. Coefficients c_1 and b_1 in (3) are determined from the boundary conditions at the nanoparticle surface, similar to [16, 17, 20, 21].

The main parameter in the simulation is the complex index of refraction of the metal. Its values were adopted from [22].

RESULTS OF CALCULATIONS

The dependences of extinction efficiency Q_{ext} on radius R calculated from expressions (1)–(3) for silver, gold, nickel, and aluminum nanoparticles in a transparent matrix with $m_0 = 1.5$ are illustrated in Fig. 1. The spectral dependences of the extinction and absorption efficiencies of silver, gold, nickel, and aluminum nanoparticles are presented in Figs. 2 and 3,

Table 2. Calculated position and amplitude of peaks in the spectral dependence of absorption, scattering, and extinction efficiency coefficients for nickel and aluminum nanoparticles of different radii

R, nm	Nickel						Aluminum					
	λ_1, nm	Q_1	λ_2, nm	Q_2	λ_3, nm	Q_3	λ_1, nm	Q_1	λ_2, nm	Q_2	λ_3, nm	Q_3
50	521.8	1.89	515.3	1.94	517.6	3.83	512.0	0.63	465.1	4.20	468.1	4.82
55	564.2	1.75	540.2	2.10	545.7	3.84	587.7	0.60	500.6	3.97	505.5	4.51
60	371.5	1.71	593.6	2.22	596.8	3.85	619.8	0.58	535.5	3.79	543.3	4.29
65	391.7	1.69	636.9	2.35	635.8	3.86	804.7	0.60	563.2	3.61	574.8	4.09
70	408.3	1.65	664.7	2.44	667.1	3.85	820.9	0.64	594.5	3.45	607.5	3.92
75	423.8	1.61	697.6	2.49	705.2	3.81	835.1	0.66	628.2	3.30	643.3	3.77
80	441.4	1.56	734.8	2.53	745.6	3.78	846.8	0.67	657.9	3.17	686.4	3.64
85	461.4	1.51	766.7	2.55	783.2	3.74	855.2	0.67	702.0	3.06	736.7	3.56
90	371.7	1.47	800.6	2.55	821.3	3.70	860.5	0.65	745.5	2.98	788.7	3.51
95	381.4	1.45	841.0	2.55	864.1	3.66	863.7	0.62	775.5	2.90	871.3	3.50
100	391.0	1.43	894.9	2.55	912.3	3.63	865.2	0.59	936.3	2.96	890.0	3.50

respectively. Position of peaks and their amplitudes, including scattering efficiencies for silver and gold, are also listed in Table 1. For nickel and aluminum, parameters of the first local maximum on the curves, appearing with decreasing the wavelength of light, are listed in Table 2. The following notations were used in Tables 1 and 2: λ_1, λ_2, and λ_3 are the wavelengths corresponding to the peaks in the $Q_{abs}(\lambda)$, $Q_{sca}(\lambda)$, and $Q_{ext}(\lambda)$ dependences, respectively; Q_1, Q_2, and Q_3 are the amplitudes of the peaks of the absorption, scattering and extinction efficiency coefficients for nanoparticles of radius R, respectively.

Silver

It follows from the calculated dependences of the extinction efficiency on radius of silver nanoparticles (Fig. 1a) that each dependence $Q_{ext}(R)$ has a peak ($Q_{ext\ max}$), the position of which ($R_{ext\ max}$) is determined by the wavelength of light. At smaller values of radius ($R \leqslant R_{ext\ max}$), the curve descends to zero, while, at larger values of radius, it levels off, exhibiting decaying oscillations. In the case of silver nanoparticles, the highest amplitude of 10.96 is reached for nanoparticles with a radius of 36 nm on the curve calculated for the wavelength of 500 nm. An increase in the wavelength of light causes the peak to shift toward larger values of radius, e.g., a peak with amplitude of 3.72 for the wavelength of 950 nm is observed for nanoparticles with a radius of 105 nm. Note that the amplitude of the global maximum at the wavelength of 500 nm exceeds those of local peaks by more than a factor of 2, while, at other wavelengths, the amplitudes of all peaks in $Q_{ext}(R)$ dependence are comparable.

Calculated spectral dependences of the coefficients of extinction and absorption efficiency for silver nanoparticles are presented in Figs. 2a and 3a, respectively. For particles with a radius of 10 nm, the spectral band of extinction has full width at half maximum of 20 nm. With increasing radius of silver nanoparticles, the peak experiences a red shift and broadens. For instance, for particle radius of 30 nm, the extinction bandwidth exceeds 60 nm. At $R = 50$ nm, the dependence $Q_{ext}(\lambda)$ reveals two peaks of comparable amplitude. Positions of peaks of absorption, scattering, and extinction efficiency coefficients in spectral dependences are listed in Table 1. It follows from the presented data that absorption dominates over scattering for nanoparticles with a radius of 15 nm and smaller. With increasing radius, the wavelength at which the scattering efficiency attains maximum for a given type of nanoparticles monotonically increases. In contrast, the dependence of position of the peaks of absorption and scattering efficiencies in the spectrum on radius of nanoparticles is not monotonic: the wavelength, at which absorption efficiency reaches maximum, drastically decreases at 40–42 nm. A similar decrease in the wavelength, at which coefficient of extinction efficiency attains maximum, occurs later, for nanoparticles with a radius of 45–47 nm. To explain the nature of the drastic change in the position of peaks of absorption and extinction efficiency coefficients with an increase in the silver nanoparticles' radius, we calculated contributions of the main harmonics to extinction and scattering efficiencies for silver nanoparticles of radius 10 and 50 nm from Eqs. (3) and (4). The results are presented in Figs. 4a, 4b and 4c, 4d, respectively. The diagrams show that only the first electric oscillation, c_1, is relevant for small nanoparticles. In the case of nanoparticles of 50-nm radius, the two first electric oscillations, c_1 and c_2, already make comparable contributions to light scattering and extinction. As a result, there appears an additional maximum in the blue spectral region. The difference

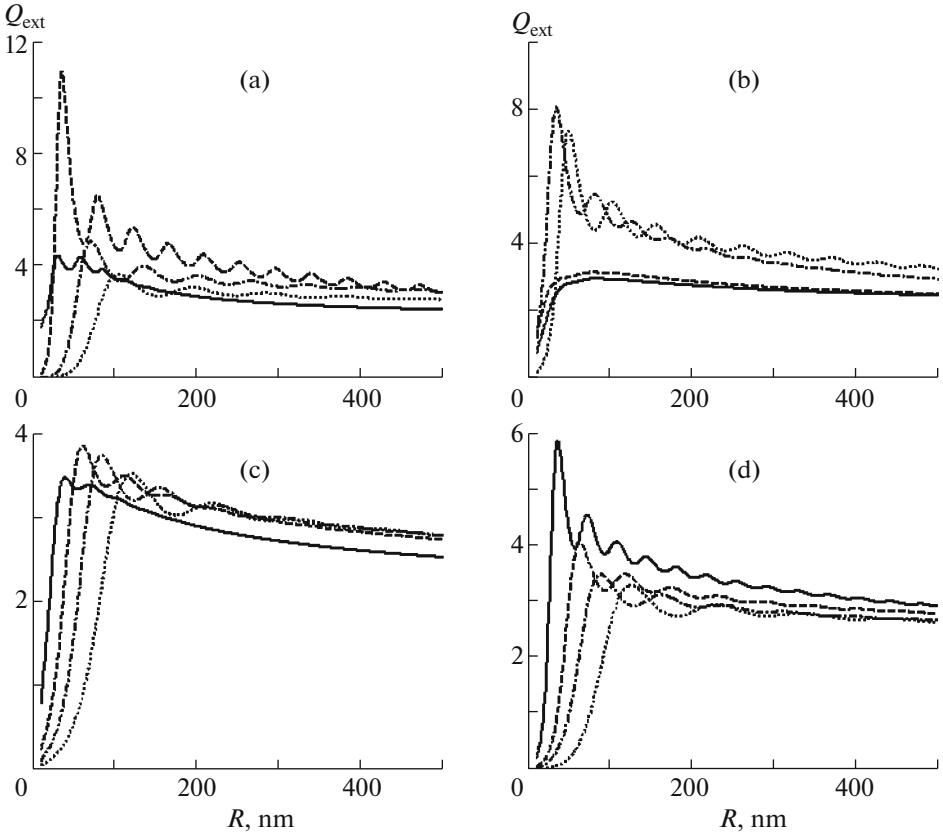

Fig. 1. Calculated dependences of light extinction efficiency on nanoparticle radius for nanoparticles of (a) silver, (b) gold, (c) nickel, and (d) aluminum. The corresponding wavelengths (nm) are (a) 400 (solid line), 500 (dashed line), 700 (dash-dotted line), and 950 (dotted line); (b) 450 (solid line), 500 (dashed line), 550 (dash-dotted line), and 600 (dotted line); and (c, d) 400 (solid line), 600 (dashed line), 800 (dash-dotted line), and 1100 (dotted line).

of spectral dependences $F^c_{l\,\mathrm{ext}}$ and $F^c_{l\,\mathrm{sca}}$ yields the spectral dependence of harmonic contributions to the absorption efficiency. It can be seen from Figs. 3a, 4c, and 4d that light absorption by silver nanoparticles of 50-nm radius is caused by two plasmon electric oscillations, c_1 and c_2, simultaneously, which explains the shift of maximum in the spectral dependence of the absorption and extinction efficiency coefficients to the blue spectral region.

Gold

The calculated dependence $Q_{\mathrm{ext}}(R)$ for gold nanoparticles is illustrated in Fig. 1b. The character of dependences calculated for the wavelengths of 400 and 450 nm differs from those obtained for 550 and 600 nm. In the first case, the dependence reveals a very flat maximum (a plateau), while, in the second case, the first maximum dominates on the curves, similarly to the results obtained for silver nanoparticles (Fig. 1a). At the wavelength of 450 nm, the peak with amplitude of 2.96 corresponds to nanoparticle radius of 83 nm, while, at 550 nm, the peak amplitude increases to 8.07, and the peak itself shifts to the position corresponding to nanoparticle radius of 34 nm. With increasing wavelength, the position of the global maximum changes nonmonotonically, shifting first to the area corresponding to smaller values of radius and then to the area corresponding to larger values of radius.

Spectral dependences of the extinction and absorption efficiency coefficients calculated for gold nanoparticles are presented in Figs. 2b and 3b, respectively. For each of the studied values of radius, there are narrow bands of extinction and absorption with a typical width of about 50 nm. With increasing radius, the peaks experience a red shift. For larger values of nanoparticle radius, the spectral dependence of the extinction efficiency broadens, while the corresponding dependence for the absorption efficiency loses its structure (Figs. 2b and 3b, the curve corresponding to 50 nm). The positions of peaks of the absorption, scattering, and extinction efficiency coefficients in spectral dependences are presented in Table 1. It follows from Table 1 that absorption dominates over scattering for nanoparticles with a radius smaller than 35 nm. With increasing radius, the wavelength, at which

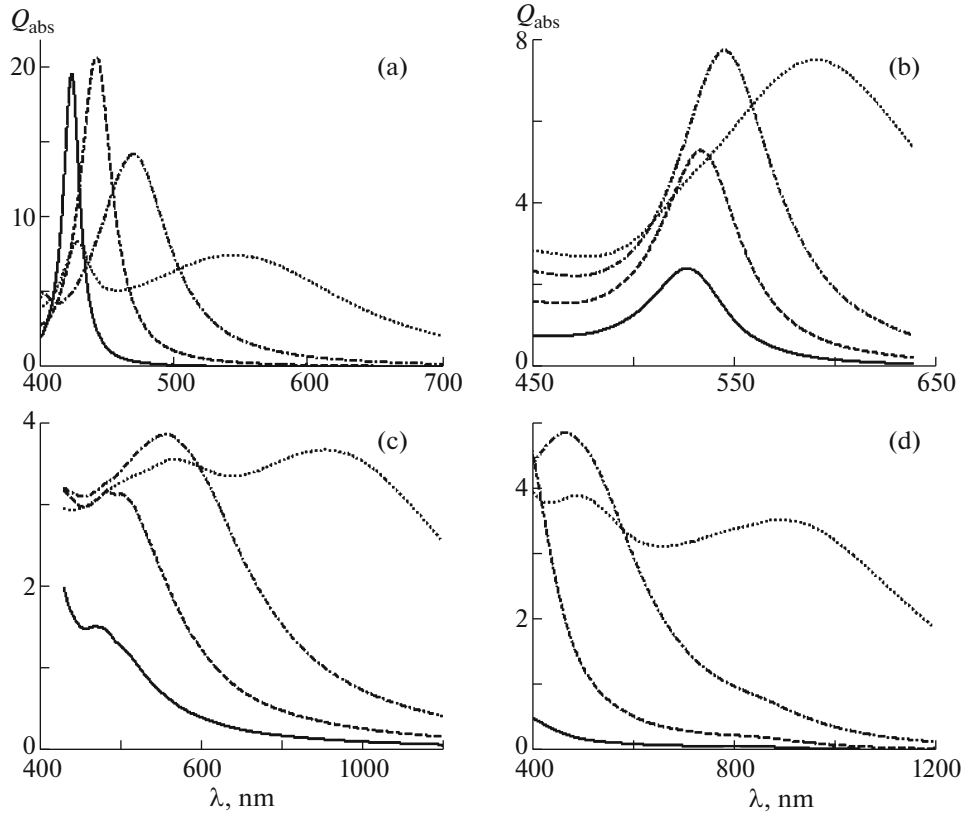

Fig. 2. Calculated spectral dependences of light extinction efficiency for nanoparticles of (a) silver, (b) gold, (c) nickel, and (d) aluminum. The corresponding values of nanoparticle radius (nm) are (a, b) 10 (solid line), 20 (dashed line), 30 (dash-dotted line), and 50 (dotted line); and (c, d) 15 (solid line), 30 (dashed line), 50 (dash-dotted line), and 100 (dotted line).

extinction and scattering efficiency coefficients attain maximum for given nanoparticles, monotonically increases. In contrast, the dependence of the absorption efficiency peak position in the spectrum on radius of nanoparticles is nonmonotonic, revealing a drastic drop in the interval between 42.5 and 45.0 nm. This drop, similarly to in the case of silver nanoparticles, is explained by the fact that the contribution of the second electric oscillation c_2 to light extinction increases with increasing nanoparticle radius. Since the peak positions in the dependences of the first harmonic contribution to absorption and extinction coincide, their difference turns out to be a slow varying function. The contribution of electric oscillation c_2 to light extinction, which does not reveal itself in scattering, becomes visible against the background of this slow dependence. The discussed contribution leads to the appearance of an additional maximum in the spectral dependence of the absorption efficiency, which is blue-shifted relative to the maximum of the extinction efficiency. In addition, the light absorption band of 50-nm gold nanoparticles becomes structureless (Fig. 3b), which was explained above.

Nickel

The $Q_{ext}(R)$ dependence calculated for nickel nanoparticles is depicted in Fig. 1c. The first local maximum has the highest amplitude on all curves. After the peak, the extinction efficiency decreases. For wavelengths of 600 nm and longer, the descending part of the curve reveals damped oscillations, which are less pronounced at the wavelength of 400 nm. The peak amplitude weakly depends on wavelength, varying in the interval from 3.47 to 3.85. With increasing wavelength, the peak shifts toward larger values of the radius approximately as $R_{ext\ max} \sim \lambda$.

The calculated dependences of extinction and absorption efficiency coefficients for nickel nanoparticles imbedded in a matrix with an index of refraction equal to 1.5 are presented in Figs. 2c and 3c, respectively. Calculations were made for the wavelength interval from 260 to 1200 nm. The dependences for nickel nanoparticles with a radius of 15 nm show mainly a decrease in absorption and extinction efficiencies. There is a small local maximum at 342 nm in the wavelength dependence of the absorption efficiency. In this interval of nanoparticle radii, absorption dominates in the entire studied wavelength range.

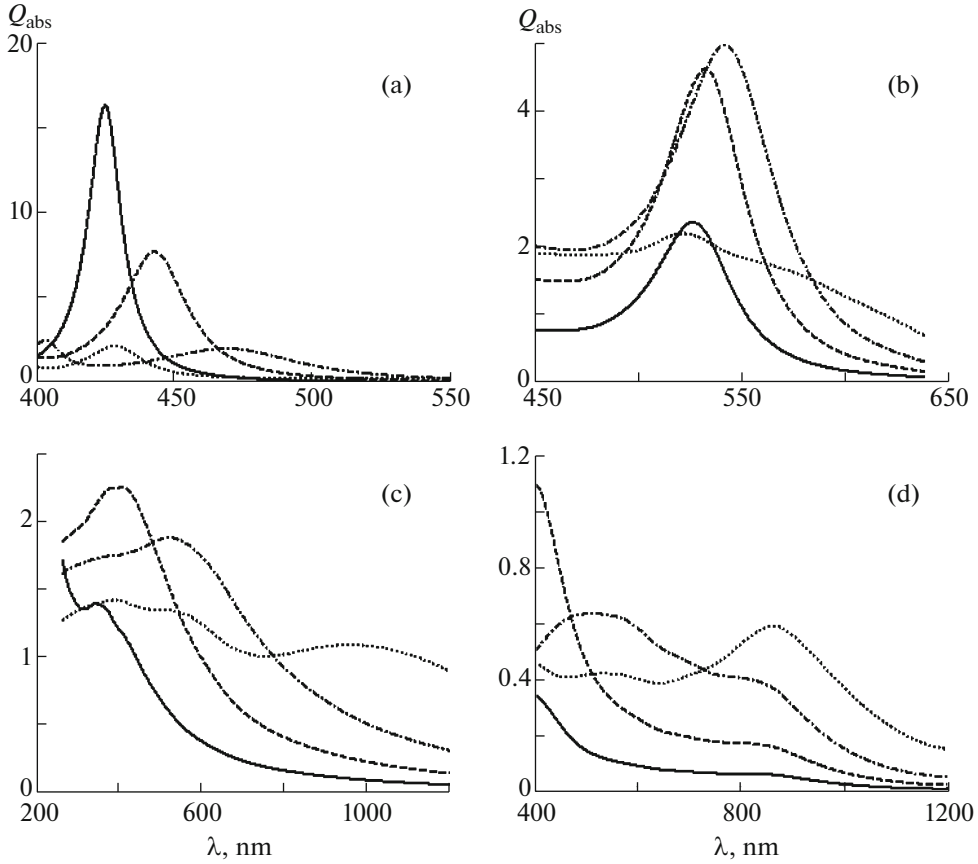

Fig. 3. Calculated spectral dependences of light absorption efficiency for nanoparticles of (a) silver, (b) gold, (c) nickel, and (d) aluminum. The corresponding values of nanoparticle radius are the same as in Fig. 2.

An absorption band with a maximum at 522 nm and characteristic bandwidth of 250 nm is observed in the wavelength dependence of the absorption efficiency corresponding to nickel nanoparticles with a radius of 50 nm. The peak in the dependence of extinction efficiency is shifted relative to the peak of absorption efficiency and lies at 517.6 nm. With increasing nanoparticle radius, the value of $Q_{\text{abs max}}$ shifts to the red spectral region. In so doing, there appear additional high-amplitude peaks in the blue spectral region. The peak of scattering efficiency also experiences a red shift with increasing nanoparticle radius. Comparison of the position of the first maximum located in the red spectral region with wavelength allows drawing a conclusion that the following relation holds approximately: $\lambda_{\max}(R)/R \approx \text{const}$.

To interpret the nature of the peaks, we calculated contributions of electric and magnetic oscillations to light absorption and extinction by nickel nanoparticles. The sample dependences calculated for nickel nanoparticles of a radius of 50 nm are presented in Figs. 4e and 4f. The contribution of the first electric oscillation c_1 attains a maximum the position of which coincides with that of the peaks of extinction and absorption. In the vicinity of the maximum, the contribution of this oscillation exceeds contributions of all other electric and magnetic oscillations by approximately a factor of 10.

Aluminum

The dependences of the light extinction efficiency on radius of nanoparticles for several wavelengths are presented in Fig. 1d. With increasing wavelength, the peak amplitude decreases from 5.87 ($\lambda = 400$ nm) to 3.30 ($\lambda = 1100$ nm). Simultaneously, the peak position as a function of nanoparticle radius shifts from 36 to 126 nm.

Spectral dependences of the extinction and absorption efficiency coefficients calculated for aluminum nanoparticles are presented in Figs. 2d and 3d, respectively. For smaller values of nanoparticle radius, 15 and 30 nm, the extinction and absorption efficiency coefficients monotonically decrease with increasing wavelength. For nanoparticles with a radius of 50 nm, spectral dependence of the extinction efficiency reveals one maximum, while that for nanoparticles with a radius of 100 nm has two maxima. The appearance of maximum in the blue spectral region is related

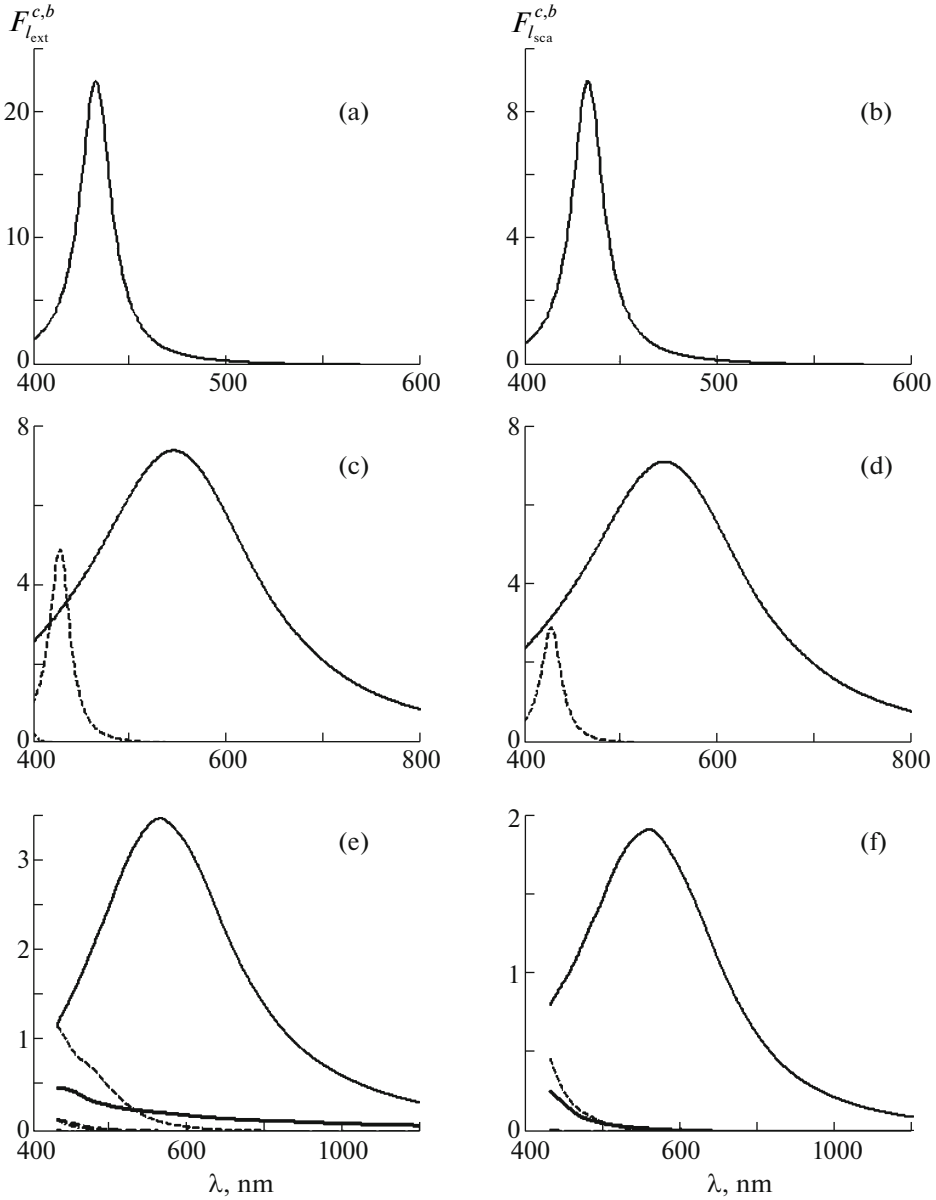

Fig. 4. Calculated spectral dependences of contributions of harmonics to light extinction (a, c, e) and scattering (b, d, f) by nanoparticles of silver with a radius of (a, b) 10 and (c, d) 50 nm and nickel with a radius of 50 nm (e, f): c_1 (thin solid line), c_2 (thin dashed line), c_3 (thin dash-dotted line), b_1 (thick solid line), b_2 (thick dashed line), and b_3 (thick dash-dotted line).

to contribution of several electric and magnetic oscillations, whereas, for nanoparticles of small radius, the dependence is determined solely by the first electric oscillation c_1. According to Table 2, the first local maximum in spectral dependences of the extinction and absorption efficiency coefficients shifts to the red spectral region, which is approximately proportional to the nanoparticle radius.

Hence, several specific features of light absorption by metal nanoparticles of different nature can be noted. The studied metals can be divided into two groups.

1. Silver and gold, for which a relatively narrow band in the spectral dependences of their optical characteristics is observed (Figs. 2a, 2b and 3a, 3b) for nanoparticles with a given radius. The peak of extinction shifts to the red spectral region with increasing radius of nanoparticles.

2. Nickel and aluminum, for which a very broad band is observed in the spectral dependences of optical characteristics (Figs. 2c, 2d and 3c, 3d). The first local minimum of extinction shifts to the red spectral region, so that $\lambda_{max}(R)/R \approx \text{const}$. Deviations from this approximate relation for the studied metals do not exceed 5%.

DISCUSSION

It should be noted that oscillation c_1 is mainly responsible for light extinction in the region of the first maximum in spectral dependence for both cases (Fig. 4). Let us formally write the expression for the extinction coefficient retaining only the first dominant term in the sum,

$$Q_{\text{ext}} \approx (6/\rho^2)\,\text{Im}\,c_1 = (3/2)(\lambda/\pi m_0 R)^2\,\text{Im}\,c_1. \quad (4)$$

Calculating the total derivative of (4) with respect to wavelength and taking into consideration spectral dependence of the complex index of refraction of a metal, we have

$$\frac{dQ_{\text{ext}}}{d\lambda} = 3\left(\frac{\lambda}{\pi m_0 R}\right)^2\left[\frac{\text{Im}\,c_1}{\lambda} + \frac{1}{2} \times\left(-\frac{2\pi m_0 R}{\lambda^2}\frac{\partial\,\text{Im}\,c_1}{\partial\rho} + \frac{\partial\,\text{Im}\,c_1}{\partial n}\frac{\partial n}{\partial\lambda} - \frac{\partial\,\text{Im}\,c_1}{\partial\kappa}\frac{\partial\kappa}{\partial\lambda}\right)\right], \quad (5)$$

The minus sign before the last term in parentheses is related to the sign in expression $m = n - i\kappa$. Let us analyze two limiting cases.

(i) The last two terms in parentheses in (5), which are related to spectral dependence of the complex index of refraction of a metal, are dominant. This effect takes place when real and imaginary parts rapidly change upon increase in wavelength. The effect can also reveal itself if derivatives $\partial n/\partial\lambda$ and $\partial\kappa/\partial\lambda$ have opposite signs. In this case, the first term in parentheses can be omitted, and position of peak in the spectral dependence of the extinction efficiency can be found from the approximate expression

$$\lambda_3 = 2\left[-\frac{\partial\ln\text{Im}\,c_1}{\partial n}\frac{\partial n}{\partial\lambda} + \frac{\partial\ln\text{Im}\,c_1}{\partial\kappa}\frac{\partial\kappa}{\partial\lambda}\right]^{-1}.$$

In this limiting case, peak position is determined mainly by spectral dependence of the complex index of refraction. It also implicitly depends on nanoparticle radius through partial derivatives of quantity $\text{Im}\,c_1(\rho)$. As an example, we can mention gold nanoparticles, for which the real part of the index of refraction decreases from 1.2543 to 0.1667 in the spectral interval between 480 and 640 nm. Simultaneously, the imaginary part of its index of refraction increases from 1.7301 to 3.6902 [22]. For gold nanoparticles, the peak in the spectral dependence of the extinction efficiency for nanoparticles the radius of which falls into the interval from 10 to 50 nm is observed in the spectral region between 527.8 and 591.5 nm; for silver nanoparticles, the peak is observed in the spectral interval between 425.2 and 524.0 nm.

In general, the results of calculation for silver agree with those found in [23]. The difference in the positions of the peaks is caused by the difference in dielectric permittivity of the medium into which nanoparticles are imbedded. The effects of variation of peak position in the spectral dependence of the extinction and absorption efficiency coefficients obtained in the present work were noted in [23]. An earlier shift of the peak of absorption efficiency to the blue spectral region relative to that of the extinction efficiency agrees with the experimental dependences obtained in [23].

(ii) Assume that the first term in parentheses on the right-hand side of (5) is dominant. Such situation can take place in the case of weak spectral dependence of the complex index of refraction. A simultaneous increase in both real and imaginary parts of the complex index of refraction of a metal, which leads to partial compensation of the last two terms in (5), also facilitates the occurrence of such situation. In this case, the position of the peak in the spectral dependence of the extinction efficiency is determined by the expression

$$\lambda_3/R = \pi m_0 \partial\ln\text{Im}\,c_1/\partial\rho. \quad (6)$$

The right-hand side of Eq. (6) is weakly dependent on wavelength through spectral dependence of $m(\lambda)$. Therefore, the position of the peak in the spectral dependence of absorption efficiency will be approximately proportional to nanoparticle radius. Of course, all the above discussions are valid only for the interval of wavelengths in which contribution of the first electric oscillation c_1, i.e., the first local maximum encountered when moving from the red to the blue spectral region, is dominant. Of the studied metals, nickel and aluminum belong to the second group. In particular, for nickel, the absolute value of the real part of the index of refraction in the spectral region from 260 to 1200 nm increases from 1.89 to 2.79, while the absolute value of the imaginary part increases from 2.30 to 6.35. It should be noted that, in the studied spectral region, the peak appears only if the radius of nanoparticles exceeds 50 nm. Otherwise, the peak should appear at shorter wavelengths. Extinction spectra of colloidal solutions of nickel were obtained in [24]. It was concluded that nickel nanoparticles 6–30 nm in size give rise to a weak extinction band (shoulder) at 350 nm [24], which agrees with the results of the calculations. Interestingly, for small-radius nickel nanoparticles, the position of the local peak of extinction is almost independent of their radius, being the same, e.g., for nanoparticles with a radius of 5, 10, and 15 nm. Hence, the above-mentioned spectral band cannot be used for determining the size of nanoparticles. This specific feature can be explained by the fact that the limiting case of the Rayleigh law can be used for nickel nanoparticles of small radius. According to this law, the extinction efficiency coefficient is described by the expression

$$Q_{\text{ext}} = 8\pi\frac{Rm_0}{\lambda}\,\text{Im}\left(\frac{1-m^2}{2+m^2}\right).$$

In the Rayleigh limit, the presence of the peak of $Q_{ext}(\lambda)$ can be related exclusively to specific features of the $m(\lambda)$ dependence.

Let us analyze the obtained results from the point of view of the concept of plasmon resonance of surface oscillations of electron density in nanoparticles. There are several approaches to determining plasmon resonance. One of them consists in defining contributions of different electric and magnetic oscillations to the effect and selecting the one with the largest contribution. The presence of the local maximum in the $Q_{ext}(\lambda)$ dependence does not necessarily correspond to one type of oscillation. It can be seen from Fig. 3b that the first maximum in the red spectral region corresponds to nearly pure oscillation c_1, whereas the peak in the blue spectral region forms due to comparable with each other contributions of several oscillations. The second approach proposed in [19] is based on finding the conditions that make the denominator zero in expressions (4) with the help of frequency dependence of the complex index of refraction of the metal, which follows from Drude model. In this approach, the frequency turns out to be complex. Since we used the experimental dependence of the index of refraction on wavelength, we can use only the first approach. Within the framework of this approach, both cases analyzed above can be associated with plasmon resonance. Both cases clearly show the dominance of one type of eigenoscillation (c_1) in absorption, despite different structure of the spectral dependences and the range of radii of nanoparticles in which they appear.

Simultaneous presence of several electric and magnetic oscillations can be seen in the dependences of extinction efficiency on radius of nanoparticles at constant wavelength of light (Fig. 1). As a rule, oscillation c_1 dominates before the first maximum. In the case of silver nanoparticles, at the wavelength of 500 nm, this oscillation forms the first peak due to fulfillment of the plasmon resonance conditions, which explains the higher amplitude of global maximum relative to other local maxima in the $Q_{ext}(R)$ dependence. The contributions of a large number of harmonics to light extinction by gold nanoparticles at the wavelengths of 450 and 500 nm and radius $R > 70$ nm become comparable, causing the appearance of a broader maximum that is close to a plateau.

In addition, the obtained dependences allow drawing a conclusion regarding the applicability of spectral measurements for finding the radius of nanoparticles of different metals. Obtaining the radius of noble metal nanoparticles from the spectral dependence of the extinction coefficient is a classical technique. However, the results obtained in the present work suggest that the variety of metals to which such an approach is applicable is limited. The radius of nanoparticles of such metals as nickel and aluminum cannot be measured if it is smaller than 50 nm. The applicability of the technique to particles of larger radius for such metals is also doubtful due to the large spectral bandwidth, which reduces the correctness of formulation of the inverse problem.

CONCLUSIONS

In the present work, we calculated spectral dependences of the light extinction and absorption efficiency coefficients for silver, gold, nickel, and aluminum nanoparticles. We demonstrated that, for nanoparticles of small radius, the contribution of the first electric oscillation associated with plasmon resonance to extinction and absorption efficiency is dominant. At large values of nanoparticle radius, the contribution of higher-order oscillations becomes evident. The differences between plasmon resonance the bands of nanoparticles of noble metals, nickel, and aluminum are revealed. In the case of noble metals, narrow plasmon resonances are observed for nanoparticles of small radius (less than 50 nm), while, for nickel and aluminum nanoparticles, broad bands in the spectral dependences of extinction and absorption efficiency coefficients are typical. The obtained results show that using the spectral dependences of the extinction coefficient for estimating radius of nanoparticles is correct only in the case of noble metals. The observed differences are related to the character and rate of changes in the real and imaginary parts of the index of refraction with increasing wavelength.

ACKNOWLEDGMENTS

We are grateful to Prof. Yu.A. Zakharov, corresponding member of the Russian Academy of Sciences, for useful discussions that stimulated this research.

This work was partially supported by the Russian Foundation for Basic Research (project no. 14-03-00534A), the grant of Russian Federation president (MK-4331.2015.2), and by the Russian Ministry of Education and Science (state assignment no. 2014/64).

REFERENCES

1. A. I. Ryasnyanskiy, B. Palpant, S. Debrus, U. Pal, and A. L. Stepanov, Phys. Solid State **51**, 55 (2009).
2. W. Husinsky, A. Ajami, P. Nekvindova, B. Svecova, J. Pesicka, and M. Janecek, Opt. Commun. **285** (10–11), 2729 (2012).
3. Y. H. Wang, X. X. Yu, F. Liu, and Y. M. Wang, Mater. Lett. **123**, 35 (2014).
4. M. Kumar, C. S. S. Sandeep, G. Kumar, Y. K. Mishra, R. Philip, and G. B. Reddy, Plasmonics **9** (1), 129 (2014).
5. P. Lama, A. Suslov, A. D. Walser, and R. Dorsinville, Opt. Express **22** (11), 14014 (2014).
6. Y. H. Wang, Y. M. Wang, J. D. Lu, L. L. Ji, R. G. Zang, and R. W. Wang, Opt. Commun. **283** (3), 486 (2010).

7. S. Mohapatra, Y. K. Mishra, A. M. Warrier, R. Philip, S. Sahoo, A. K. Arora, and D. K. Avasthi, Plasmonics **7** (1), 25 (2012).
8. V. E. Kaidashev, N. V. Lyanguzov, Yu. I. Yuzyuk, and E. M. Kaidashev, Tech. Phys. **57** (10), 1406 (2012).
9. V. I. Kukushkin, A. B. Van'kov, and I. V. Kukushkin, JETP Lett. **98** (6), 342 (2013).
10. E. Moulin, J. Sukmanowski, M. Schulte, A. Gordijn, F. X. Royer, and H. Stiebig, Thin Solid Films **516** (20), 6813 (2008).
11. M. Karami, M. Raisee, and S. Delfani, Opt. Spectrosc. **115** (3), 400 (2013).
12. V. K. Pustovalov and L. G. Astafyeva, Las. Phys. **21** (12), 2098 (2011).
13. L. A. Dombrovsky, V. Timchenko, M. Jackson, and G. H. Yeoh, Int. J. Heat Mass Transfer **54** (24–26), 5459 (2011).
14. A. V. Kalenskii, A. A. Zvekov, M. V. Anan'eva, I. Yu. Zykov, V. G. Kriger, and B. P. Aduev, Comb. Expl. Shock Waves **50** (3), 333 (2014).
15. B. P. Aduev, D. R. Nurmukhametov, R. I. Furega, and A. A. Zvekov, Rus. J. Phys. Chem. B **8** (3), 352 (2014).
16. B. P. Aduev, D. R. Nurmukhametov, R. I. Furega, A. A. Zvekov, and A. V. Kalenskii, Rus. J. Phys. Chem. B **7** (4), 453 (2013).
17. V. G. Kriger, A. V. Kalenskii, A. A. Zvekov, I. Yu. Zykov, and B. P. Aduev, Comb. Expl. Shock Waves **48** (6), 705 (2012).
18. B. P. Aduev, M. V. Anan'eva, A. A. Zvekov, A. V. Kalenskii, V. G. Kriger, and A. P. Nikitin, Comb. Expl. Shock Waves **50** (6), 704 (2014).
19. K. Kolwa, A. Derkachova, and M. Shopa, J. Quant. Spectrosc. Radiat. Transfer **110** (14–16), 1490 (2009).
20. K. S. Shifrin, *Light Scattering in Turbid Media* (Gos. Tekh. Izdat., Moscow, 1951) [in Russian].
21. N. V. Malimonenko, I. S. Dudkin, and B. Ya. Kogan, Opt. Spectrosc. **116** (3), 424 (2014).
22. V. M. Zolotarev, V. N. Morozov, and E. V. Smirnov, *Optical Constants of Natural and Technical Media* (Khimiya, Leningrad, 1984) [in Russian].
23. D. D. Evanoff, Jr., and G. Chumanov, Chem. Phys. Chem. **6** (7), 1221 (2005).
24. B. G. Ershov, Zh. Ros. Khim. Ob-va **45** (3), 20 (2001) [in Russian].